

**On the local instability of radial hedgehog configurations
in nematic liquid crystals
under Landau-de Gennes free-energy models**

E. C. Gartland, Jr.*

Department of Mathematics and Computer Science, Kent State University, Kent, OH 44242

S. Mkaddem[†]

UGRU, UAE University, Al-Ain, Abu Dhabi, United Arab Emirates

(July 14, 1998 original; November 5, 1999 revised)

Abstract

We consider radial hedgehog equilibrium configurations of the tensor order parameter in spherical droplets of nematic liquid crystals modeled by free energies of Landau-de Gennes type. We show that such configurations must cease to be metastable at sufficiently low temperatures in droplets of sufficiently large radii for all but a very limited range of elastic-constant ratios, which are very near the limit where the elastic-energy terms in the model cease to be positive definite. The analysis is complicated by the fact that no analytical solution is available for the hedgehog configuration. Nevertheless, using a combination of analytical bounds and numerical computation, we are

*Also affiliated with Chemical Physics Interdisciplinary Program, Liquid Crystal Institute, Kent State University, Kent, OH, USA. Electronic address: gartland@mcs.kent.edu

[†]Electronic address: smkaddem@uaeu.ac.ae

able to construct a perturbation to which we can show that the spherically symmetric ground state loses its local stability.

61.30.Gd, 61.30.Jf, 64.70.Md

I. INTRODUCTION

The study of equilibrium structures and defects of confined liquid crystals has been an area of interest for some time. Here we consider spherical droplets of a nematic with radial strong-anchoring conditions modeled by a Landau-de Gennes tensor-order-parameter model. We are motivated primarily by the succession of papers [1–4]. In [1] Schopohl and Sluckin illustrated for this problem the structure of a radial hedgehog configuration with an isotropic core. Penzenstadler and Trebin [2] then showed that the core should instead broaden to a small ring (or loop) disclination (of 180° or strength $1/2$). This was validated numerically by Sonnet, Kilian, and Hess in [3]. Rosso and Virga [4] argued that the radial hedgehog solution remained at least metastable over a certain range. Related results are presented in [5–7].

Motivated by this evolution of thought, we have undertaken a detailed numerical investigation of this system, on which we will report elsewhere. In the numerical modeling of the full system, we have imposed *rotational symmetry*. In addition to the (spherically symmetric) radial hedgehog and the (axially symmetric) ring disclination solutions, we found a new, metastable configuration, which also is axially symmetric and which consists of a “split core” with two isotropic points narrowly separated by a line disclination segment along the rotational symmetry axis. The three solutions, which coexist over a broad range of parameters, are depicted in Figure 1. These structures all are quite small, existing within a distance from the center of the droplet that is on the order of tens of units of the size of the hedgehog core.

We have computed a bifurcation diagram, Figure 2, that indicates how these solutions are connected to each other. Since all three of these tensor fields are forced by symmetry to be *uniaxial* along their rotational symmetry axes (in particular at the center of the droplet), the nature of their orientational order at the *center* can be characterized by the value of the *scalar order parameter* there. We have used this as a parameter to distinguish the branches of equilibrium solutions in Figure 2. This figure is reflective of the common situation of an

“imperfect bifurcation,” in which the transcritical bifurcation point of the true (continuous) problem has separated under discretization into two nearby but distinct branches.

The diagram indicates that at a certain *critical temperature*, the radial hedgehog solution branch becomes locally unstable (not metastable), and off of it bifurcate two branches, which break the spherical symmetry (to axial symmetry). The lower, metastable branch corresponds to the *split core* solution, which is uniaxial with a *negative* order parameter at the center; while the upper branch corresponds to the *ring disclination*, which is uniaxial with a *positive* order parameter at the center, and which does not become metastable until the radius of the ring grows to sufficient size. Such a bifurcation diagram is typical for this kind of weak first-order structural phase transition, which is found to be common in such liquid crystal systems. It very much resembles the bifurcation diagram for the nematic-to-isotropic transition in the bulk.

Guided by this numerical evidence, we have developed a direct argument (which we present here) that the hedgehog solution must become locally unstable for sufficiently low temperature provided that the radius of the droplet is sufficiently large and that the elastic constants in the model are not too close to a certain limiting point of their admissible values. We demonstrate the instability by explicitly constructing a perturbation to which we can show that the radial hedgehog loses its metastability. The analysis is complicated by the fact that there is no analytical solution available for the hedgehog configuration under Landau theory. We rely instead on analytical bounds and numerical solutions. We mention that while the numerical modeling that underlies Figure 2 imposed rotational symmetry, the analysis that follows here does not make any such assumption.

II. MODEL AND SCALINGS

Consider a Landau-de Gennes expansion of the free energy in powers of the tensor order parameter \mathbf{Q} and its gradient:

$$\mathcal{F} := \int (f_{\text{el}} + f_{\text{v}}) dV ,$$

where the *elastic* and *bulk* free-energy densities are given by

$$f_{\text{el}} := \frac{L_1}{2} Q_{\alpha\beta,\gamma} Q_{\alpha\beta,\gamma} + \frac{L_2}{2} Q_{\alpha\beta,\beta} Q_{\alpha\gamma,\gamma} + \frac{L_3}{2} Q_{\alpha\beta,\gamma} Q_{\alpha\gamma,\beta}$$

and

$$f_{\text{v}} := \frac{a}{2} \text{tr}(\mathbf{Q}^2) - \frac{b}{3} \text{tr}(\mathbf{Q}^3) + \frac{c}{4} \text{tr}(\mathbf{Q}^2)^2 .$$

The elastic constants L_1 , L_2 , and L_3 must satisfy the following conditions in order for the elastic part of the free energy to be properly positive definite (see for example [8] or [9]):

$$L_1 > 0, \quad -L_1 < L_3 < 2L_1, \quad 6L_1 + 10L_2 + L_3 > 0. \quad (1)$$

We non-dimensionalize this model in terms of the length scale $\xi := \sqrt{27cL_1/b^2}$ and rescaled variables

$$\tilde{\mathbf{r}} := \frac{\mathbf{r}}{\xi}, \quad \tilde{\mathbf{Q}} := \sqrt{\frac{27c^2}{2b^2}} \mathbf{Q}, \quad \tilde{\mathcal{F}} := \sqrt{\frac{27c^3}{4b^2L_1^3}} \mathcal{F}.$$

In terms of these (after dropping the tildes), the densities take the form

$$f_{\text{el}} = \frac{1}{2} Q_{\alpha\beta,\gamma} Q_{\alpha\beta,\gamma} + \frac{\eta_2}{2} Q_{\alpha\beta,\beta} Q_{\alpha\gamma,\gamma} + \frac{\eta_3}{2} Q_{\alpha\beta,\gamma} Q_{\alpha\gamma,\beta}$$

and

$$f_{\text{v}} = \frac{t}{2} \text{tr}(\mathbf{Q}^2) - \sqrt{6} \text{tr}(\mathbf{Q}^3) + \frac{1}{2} \text{tr}(\mathbf{Q}^2)^2 ,$$

where

$$\eta_2 := \frac{L_2}{L_1}, \quad \eta_3 := \frac{L_3}{L_1}, \quad t := \frac{27ac}{b^2}.$$

The important dimensionless parameters, then, are the *elastic-constant ratios* η_2 and η_3 , *reduced temperature* t , and the *radius* of the droplet in units of ξ , which we will denote by R .

These units were chosen to permit easy comparison with [1–4]. The length scale ξ is comparable to the correlation lengths utilized in [1,3]. In terms of t , the critical values in

the bulk are $t = 0$ (“pseudo-critical temperature,” below which the isotropic phase is not metastable), $t = 1$ (nematic-isotropic transition temperature or “clearing point”), and $t = 9/8$ (“super-heating limit,” above which the ordered phase does not exist). The conditions (1) on the elastic constants become

$$-1 < \eta_3 < 2, \quad 6 + 10\eta_2 + \eta_3 > 0. \quad (2)$$

There is a well-known “elastic constant degeneracy” associated with this model. The L_2 term (in the elastic free-energy density f_{el}) can be transformed into the L_3 term via integration by parts; their contributions to the free energy differ by a quantity that depends only on the boundary values of \mathbf{Q} on the surface of the droplet—this quantity will thus be a constant for the case of strong anchoring, which we consider here. Equilibrium configurations depend only on the sum $L_2 + L_3$. This manifests itself when comparing to the Frank model, under the assumption that \mathbf{Q} is uniaxial, where one finds

$$K_{11} = K_{33} \propto L_1 + \frac{L_2 + L_3}{2}, \quad K_{22} \propto L_1. \quad (3)$$

Because of this, it is common to work with a two-constant model and take $L_3 = 0$ —for example this is done in [2]. By contrast, in [3] a one-constant model (with $L_2 = L_3 = 0$ and $K_{11} = K_{22} = K_{33}$) is considered. Here we retain all three elastic constants, as is also done in [4], and we shall see (as was seen there) that this leads to additional possibilities when considering questions of metastability of equilibria.

III. HEDGEHOG SOLUTION

The radial hedgehog solution is distinguished by its complete spherical symmetry. It can be represented in spherical coordinates in the form

$$\mathbf{H}(r, \theta, \phi) = \sqrt{\frac{3}{2}} h(r) \left(\hat{\mathbf{e}}_r \otimes \hat{\mathbf{e}}_r - \frac{1}{3} \mathbf{I} \right). \quad (4)$$

Here the normalization has been chosen so that $\text{tr}(\mathbf{H}^2) = h^2$. Substituting this ansatz into the expression for the free energy and performing the integration with respect to $\sin\theta d\theta d\phi$

over the azimuthal and polar angles, one obtains the following expression for the free energy of a droplet of radius R :

$$\mathcal{F}(\mathbf{H}) = 4\pi \int_0^R \left\{ \frac{1}{2} \left(1 + \frac{2}{3} \eta_{23} \right) \left[(h')^2 + \frac{6}{r^2} h^2 \right] + g(h) \right\} r^2 dr + 2\pi (2\eta_2 - \eta_3) R h(R)^2,$$

where

$$\eta_{23} := \eta_2 + \eta_3 = \frac{L_2 + L_3}{L_1} \quad \text{and} \quad g(h) := \frac{t}{2} h^2 - h^3 + \frac{1}{2} h^4.$$

We mention that we have relied upon the symbolic-computation package Maple V for help with some of the more complicated derivations and formula manipulations, such as the integral expression above.

Much of what develops with the solution $h(r)$ is driven by the double-well potential $g(h)$, which is plotted in Figure 3. The function $g(h)$ depends on the reduced-temperature parameter t , and it has a negative relative minimum, at a certain value $h_- < 0$, for $t < 0$. For $t < 1$ its *global* minimum occurs at

$$h_+ := \frac{3 + \sqrt{9 - 8t}}{4}, \tag{5}$$

which is always *positive*.

The Euler-Lagrange equation for equilibrium is given by

$$\left(1 + \frac{2}{3} \eta_{23} \right) \left(h'' + \frac{2}{r} h' - \frac{6}{r^2} h \right) - g'(h) = 0, \tag{6}$$

where $g'(h) = t h - 3h^2 + 2h^3$. This is equivalent to [1, eqn. (8)] in our slightly different units. Spherical symmetry forces $h(0) = h'(0) = 0$. We will seek solutions of this singular nonlinear ordinary differential equation that satisfy the additional condition $h(R) = h_+$ or the limiting form of this, $h(\infty) = h_+$.

Intuitively one can see the reason why the radial hedgehog solution might become locally unstable. Symmetry is forcing h to be *zero* at the center; whereas the potential $g(h)$ would prefer the value $h = h_+$ (or at least $h = h_-$)—provided that one can accommodate this with respect to the elastic energy contributions.

An analytical solution for (6) is not available. For this reason, in other analyses of this and related problems, it is common to approximate $h(r)$ by an “outer solution,” with a point-defect singularity and $h(r)$ constant, and to analyze the relative stability or metastability of the associated tensor field \mathbf{H} —for example this is what is done in [2] and [4]. Here we propose to deal with the true solution $h(r)$ of (6). It is not hard to obtain accurate numerical solutions to this equation, and these are utilized below. Also, one can use analytical techniques involving “differential inequalities” to obtain upper and lower bounds for the solution. These provide useful information about the behavior of the solution $h(r)$, and they prove to be adequate to demonstrate its instability over a large portion of the parameter space. We discuss this now.

The *Method of Differential Inequalities* generalizes the *Maximum Principle* for differential equations. It enables one to prove existence of and to construct a-priori bounds for solutions of certain classes of problems. For our problem, a-priori bounds obtainable from standard maximum principles can be used for a rigorous metastability analysis [10], but they provide less precise information about the positive $h(r)$ solution that we characterize now. Consider a two-point boundary value problem of the general form

$$\begin{aligned} y'' &= f(t, y, y'), & a < t < b, \\ y(a) &= A, & y(b) = B. \end{aligned} \tag{7}$$

Suppose that one is able to obtain smooth functions $\alpha(t)$ and $\beta(t)$ that satisfy $\alpha(t) \leq \beta(t)$, for $a < t < b$, and

$$\begin{aligned} \alpha'' &\geq f(t, \alpha, \alpha'), & \alpha(a) \leq A, & \alpha(b) \leq B, \\ \beta'' &\leq f(t, \beta, \beta'), & \beta(a) \geq A, & \beta(b) \geq B. \end{aligned}$$

Such functions are called “lower” and “upper solutions.” If f is sufficiently regular and satisfies certain growth conditions with respect to its third argument, then one can conclude that there exists a solution $y(t)$ of (7) satisfying $\alpha(t) \leq y(t) \leq \beta(t)$ (see for example [11] or [12]).

Guided by analysis of the local behavior $h(r) = O(r^2)$, as $r \rightarrow 0$, and $h(r) = h_+ - O(1/r^2)$, as $r \rightarrow \infty$, we construct lower/upper solutions to (6) in the form

$$\alpha(r) = h_+ \frac{r^2}{r^2 + \lambda_\alpha^2} \quad \text{and} \quad \beta(r) = h_+ \frac{r^2}{r^2 + \lambda_\beta^2}, \quad (8)$$

with

$$\lambda_\alpha^2 := \left(1 + \frac{2}{3}\eta_{23}\right) \frac{14}{-t}$$

and

$$\lambda_\beta^2 := \left(1 + \frac{2}{3}\eta_{23}\right) \frac{6}{\sqrt{9-8t}} \frac{1}{h_+}.$$

One can verify directly that these satisfy the appropriate conditions. In Appendix A, we give a limiting argument to establish the validity of the bracketing $\alpha(r) \leq h(r) \leq \beta(r)$, $0 \leq r < \infty$, for our problem, which is *singular* at the origin and on an *unbounded* interval. The quality of the upper/lower bounding solutions is illustrated in Figure 4, where they are compared against a numerically computed $h(r)$ solution.

These bounding functions give the scaling of the core (or inner layer) of the hedgehog solution—this can be deduced formally from (6)—as $O(1/\sqrt{-t})$, as $t \rightarrow -\infty$. We require sharp information about the behavior of the function $h(r)$ in this limit. Motivated by the above, we seek solutions of (6) in the scaled form

$$\bar{h}(\bar{r}) = \frac{h(r)}{h_+}, \quad \bar{r} := \sqrt{\frac{-t}{1 + \frac{2}{3}\eta_{23}}} r. \quad (9)$$

Making this substitution, we obtain the rescaled differential equation

$$\bar{h}'' + \frac{2}{\bar{r}} \bar{h}' - \frac{6}{\bar{r}^2} \bar{h} + \bar{h} - \left(\frac{3h_+}{t}\right) \bar{h}^2 + \left(\frac{2h_+^2}{t}\right) \bar{h}^3 = 0. \quad (10)$$

These coefficients have the asymptotic behavior

$$\frac{3h_+}{t} = O\left(\frac{1}{\sqrt{-t}}\right), \quad \frac{2h_+^2}{t} = -1 + O\left(\frac{1}{\sqrt{-t}}\right),$$

as $t \rightarrow -\infty$. Taking this limit, we obtain the “limiting rescaled problem”

$$\begin{aligned} \hbar'' + \frac{2}{\bar{r}} \hbar' - \frac{6}{\bar{r}^2} \hbar + \hbar - \hbar^3 &= 0, \quad 0 < \bar{r} < \infty, \\ \hbar(0) &= 0, \quad \hbar(\infty) = 1. \end{aligned} \tag{11}$$

We shall denote the solution of this equation by \hbar_∞ ; in terms of it, a uniformly valid asymptotic approximation to $h(r)$ can be expressed as in (9) above. Its limiting bounding functions are

$$\bar{\alpha}_\infty(\bar{r}) := \frac{\bar{r}^2}{\bar{r}^2 + 14} \quad \text{and} \quad \bar{\beta}_\infty(\bar{r}) := \frac{\bar{r}^2}{\bar{r}^2 + 3}.$$

From the limiting behavior above, we note that for $-t$ large, the \hbar^2 term in the differential equation (10) for $\hbar(r)$ is negligible; this is consistent with the ‘‘Lyuksutov approximation’’ utilized in [2] and [4].

IV. METASTABILITY

We seek to demonstrate the loss of metastability of the radial hedgehog solution (for R and $-t$ sufficiently large) by explicitly constructing a perturbation to which it becomes locally unstable. Motivated by numerical evidence, the analyses of [2] and [4], and the desire to obtain a tractable problem, we consider tensor fields of the form $\mathbf{Q} = \mathbf{H} + \mathbf{P}$, where \mathbf{H} is the tensor field of the radial hedgehog solution, as in (4), and \mathbf{P} is a perturbation of the form

$$\mathbf{P}(r, \theta, \phi) = \sqrt{\frac{3}{2}} p(r) \left(\hat{\mathbf{e}}_z \otimes \hat{\mathbf{e}}_z - \frac{1}{3} \mathbf{I} \right).$$

Expanding $\mathcal{F}(\mathbf{H} + \mathbf{P})$ and integrating with respect to $\sin \theta d\theta d\phi$, one obtains a vanishing first variation and the following weak form of the *second variation*:

$$4\pi \int_0^R \left\{ \left(1 + \frac{1}{3} \eta_{23} \right) (p')^2 + \left[t + \frac{14}{5} h^2(r) \right] p^2 \right\} r^2 dr.$$

We will know that the hedgehog solution is locally unstable if we can construct a function $p(r)$ that produces a *negative* value for this integral. We are encouraged by the fact that in

the limit $t \rightarrow -\infty$, there is a large negative contribution from the term involving t . However, the $h^2(r)$ term is growing in this limit, and the crude estimation

$$h^2(r) < h_+^2 \sim \frac{-t}{2}, \quad \text{as } t \rightarrow -\infty,$$

is inadequate.

We normalize and recast the *local instability condition* as

$$\inf_p \frac{\int_0^R [(1 + \frac{1}{3}\eta_{23})(p')^2 + \frac{14}{5} h^2(r) p^2] r^2 dr}{\int_0^R p^2 r^2 dr} < -t,$$

where the infimum is taken over smooth functions p satisfying $p(R) = 0$. Rescaling as before in (9), renormalizing, and taking limits as $t \rightarrow -\infty$, we obtain the scaled limiting form of this condition

$$\lambda_{\min}(\varepsilon) := \inf_{\bar{p}} \frac{\varepsilon \int_0^\infty (\bar{p}')^2 \bar{r}^2 d\bar{r} + \int_0^\infty \bar{h}_\infty^2(\bar{r}) \bar{p}^2 \bar{r}^2 d\bar{r}}{\int_0^\infty \bar{p}^2 \bar{r}^2 d\bar{r}} < \frac{5}{7}, \quad (12)$$

where the ‘‘coupling coefficient’’ ε is given by

$$\varepsilon := \frac{5}{7} \frac{1 + \frac{1}{3}\eta_{23}}{1 + \frac{2}{3}\eta_{23}}.$$

This parameter is a decreasing function of η_{23} : $-3/2 < \eta_{23} < \infty \leftrightarrow \infty > \varepsilon > 5/14$. Here we have also extended the integration to the limit $R \rightarrow \infty$.

One can show that the local instability condition for finite R and t depends continuously on (ε, R, t) and that a properly scaled version of it approaches (12) in the limit as R and $-t$ approach infinity. For this, one can use the fact that the hedgehog solution $h(r)$ depends continuously on these parameters, which can be established using the continuous dependence of the solutions of ordinary differential equations on parameters and boundary conditions combined with the lower and upper bounding functions $\alpha(r)$ and $\beta(r)$ to help control the behavior near $r = 0$ and at infinity. We conclude that if the (scaled limiting) condition (12) is satisfied for some ε , then the finite local instability condition will be satisfied for all $R > R_0$ and $t < t_0$, for some R_0, t_0 , which may depend on ε .

The value $\lambda_{\min}(\varepsilon)$ corresponds to (the variational form of) a spherically symmetric Schrödinger eigenvalue problem with potential $\bar{h}_\infty^2(\bar{r})$. The form of $\bar{h}_\infty(\bar{r})$ is illustrated

in Figure 5 together with the associated principal mode $\bar{p}(\bar{r})$, which produces the minimum value in (12). The value of $\lambda_{\min}(\varepsilon)$ increases with ε , ranging over $0 < \lambda_{\min} < \infty$, for $0 < \varepsilon < \infty$. We define ε^* via $\lambda_{\min}(\varepsilon^*) = 5/7$. Then we will have $\lambda_{\min}(\varepsilon) < 5/7$ if and only if $\varepsilon < \varepsilon^*$, in which case the hedgehog tensor field \mathbf{H} will be locally unstable to a perturbation \mathbf{P} in our class.

Lower bounds for ε^* can be derived by bounding $\bar{h}_\infty(\bar{r})$ from above,

$$\bar{h}_\infty(\bar{r}) \leq \bar{\beta}_\infty(\bar{r}) = \frac{\bar{r}^2}{\bar{r}^2 + 3},$$

and evaluating the Rayleigh quotient in (12) on particular test functions $\bar{p}(\bar{r})$. After some trial and error (and numerical experimentation), we obtain the function

$$\bar{p}(\bar{r}) = \frac{1}{(\bar{r}^2 + 12)^2},$$

which somewhat mimics the principal mode of (12) (with \bar{h}_∞ replaced by $\bar{\beta}_\infty$ and $\varepsilon \approx 1$) and for which the integrals there take a simple form and give

$$\lambda_{\min}(\varepsilon) \leq \frac{\varepsilon \frac{3}{16} + \frac{28}{81}}{\frac{3}{4}}.$$

From this follows

$$\varepsilon^* \geq \frac{1724}{1701} \doteq 1.014 \quad \text{and} \quad \eta_{23}^* \leq -\frac{1527}{2233} \doteq -.684.$$

These rigorous, purely analytical estimates are sufficient to treat the two-constant ($L_3 = 0$) model, for which we must have, by virtue of the conditions (2), $\eta_{23} > -3/5$ (and as a consequence $\varepsilon < 20/21$). That is, in the $L_3 = 0$ model (as considered for example in [2]), for any admissible values of the elastic constants L_1 and L_2 , the radial hedgehog configuration must cease to be metastable at sufficiently low temperature in a droplet of sufficiently large radius.

In the full model (with L_1 , L_2 , and L_3), the restriction on the elastic-constant ratios is $\eta_{23} > -3/2$, and so the range of admissible values for ε is $5/14 < \varepsilon < \infty$. Our local instability condition must fail for ε large enough, i.e., for η_{23} sufficiently close to $-3/2$.

We resort to numerical calculations to obtain sharper estimates. We calculate $h_\infty(\bar{r})$ by solving numerically the problem (11). Using this, we then discretize the eigenvalue problem associated with (12),

$$\varepsilon \left(\bar{p}'' + \frac{2}{\bar{r}} \bar{p}' \right) + [\lambda - h_\infty^2(\bar{r})] \bar{p} = 0, \quad 0 < \bar{r} < \infty,$$

$$\bar{p}'(0) = \bar{p}(\infty) = 0,$$

and calculate the minimum eigenvalue using library software. We obtain

$$\varepsilon^* \doteq 1.720 \quad \text{and} \quad \eta_{23}^* \doteq -1.107.$$

These various regions of local instability and limits are depicted in Figure 6.

V. CONCLUSIONS

We have shown that the hedgehog equilibrium solution of a Landau-de Gennes free-energy model for a radially aligned nematic in a spherical droplet must cease to be metastable at sufficiently low temperatures and sufficiently large radii of the droplet for all but this very small region of admissible elastic constants, $-1.5 < \eta_{23} \leq \eta_{23}^*$. Our analysis was guided by results of numerical modeling of the full system and relied upon constructing an appropriate perturbation and using proper scalings to enable the extraction of a tractable local instability condition. This condition required the solution of an eigenvalue problem involving as a coefficient the unknown solution for the scalar-order-parameter field of the hedgehog, which problem was solved numerically. In addition, rigorous analytical bounds on the size of the region of local instability were obtained using guaranteed bounds on the hedgehog solution together with Rayleigh-quotient approximations.

While the particular class of perturbations we used did a reasonably good job, they did involve certain restrictions and simplifications, which were necessary in order to produce a tractable problem. The region of local instability in Figure 6 is only a “lower bound” on the true range of elastic-constant ratios for which the hedgehog will not be metastable; the

region can only grow as one broadens the class of perturbations. The analysis suggests the possibility that the radial hedgehog may in fact become locally unstable for *all* admissible values of the elastic constants.

In considering the papers that we have cited throughout, we find that our most direct comparisons can be made with [6] and [4]. In [6] Cohen and Taylor used a Frank elastic model, for which the radial hedgehog solution takes the form of the pure-splay distortion $\hat{\mathbf{n}}(r, \theta, \phi) = \hat{\mathbf{e}}_r$. They found, in terms of our parameters, that the hedgehog solution is metastable against the uniaxial perturbations admitted by Frank’s model if and only if $\eta_{23} < 2/7$. Rosso and Virga [4] considered the same Landau-de Gennes model we have used here; however, they used a certain “outer approximation” for the (unknown) hedgehog solution. They then investigated metastability with respect to particular classes of perturbations, which differ somewhat from the ones we have used here. They found the approximate hedgehog to be locally unstable (for a sufficiently large radius) if $1 + 2\eta_2 + \eta_3 > 0$. The region we obtain here contains the regions from both of these papers. Though differing in approaches (models, constraints, approximations, perturbations), the investigations share a common feature: all are unable to show loss of metastability for $(\eta_2 + \eta_3)$ “too close” to the $-3/2$ limiting value.

A feature of the analysis is the interplay between the *core* of the hedgehog and the *eigenmode* of the local instability: the eigenmode $\bar{p}(\bar{r})$ has its major content within the hedgehog core, as is illustrated in Figure 5.

Throughout this discussion, we have taken the “hedgehog solution” to be the positive solution $h(r)$ the existence of which is guaranteed by the differential-inequalities argument. Now the problem that $h(r)$ solves is nonlinear, and we are unable to preclude (at this point) the possible existence of other solutions. However, it can be shown, without much difficulty, that any other potential solution must be pointwise bounded in magnitude by $|h(r)|$, for all $0 \leq r < \infty$. So the metastability analysis of the previous section remains valid for *any* solution of the hedgehog problem. See Appendix B, where it is also shown that $h(r)$ is unique within a certain restricted class.

As a final point, we mention that while the analysis was conducted on a certain limiting problem (in the doubly infinite limit $R \rightarrow \infty$, $t \rightarrow -\infty$), the reality is that these phenomena are observed numerically for rather modest values of these variables: $R \approx 10$, $t \approx -5$ (as is seen in the figures).

ACKNOWLEDGMENTS

The authors are grateful to Professors Hans-Rainer Trebin (Stuttgart) and Epifanio G. Virga (Pavia) for their encouragement in this project. We also gratefully acknowledge the inputs of Professors Oleg D. Lavrentovich and Peter Palffy-Muhoray (Kent). This work was supported by the National Science Foundation under Grants DMR 89-20147 (ALCOM Center) and DMS-9870420 (first author).

APPENDIX A: VALIDITY OF UPPER/LOWER BOUNDS ON HEDGEHOG SOLUTION

We establish the validity of the bracketing $\alpha(r) \leq h(r) \leq \beta(r)$ of the hedgehog solution, as discussed in Section III. Expressing lengths in units of $\sqrt{1 + 2\eta_{23}/3}$, we can write the problem (6) in the cleaner form

$$h'' + \frac{2}{r}h' - \frac{6}{r^2}h - th + 3h^2 - 2h^3 = 0, \quad 0 < r < \infty, \\ h(0) = 0, \quad h(\infty) = h_+, \quad (\text{A1})$$

where $h_+ = h_+(t) > 0$ is defined in (5). Let us introduce the following notation for the nonlinear differential operator that defines this problem:

$$N[h] := h'' + \frac{2}{r}h' - \frac{6}{r^2}h - th + 3h^2 - 2h^3.$$

We first construct lower and upper solutions, $\alpha(r)$ and $\beta(r)$, that satisfy $\alpha(r) \leq \beta(r)$, $\alpha(0) = \beta(0) = 0$, $\alpha(\infty) = \beta(\infty) = h_+$, $N[\alpha] \geq 0$, and $N[\beta] \leq 0$. We seek these in the general form

$$w(r; \lambda) = h_+ \frac{r^2}{r^2 + \lambda^2},$$

for which we obtain

$$N[w] = -\frac{1}{16} \frac{(3 + \sqrt{9 - 8t}) r^2 C(r; \lambda)}{(r^2 + \lambda^2)^3},$$

where $C(r; \lambda) := A(\lambda) + B(\lambda) r^2$, with

$$A(\lambda) := 4\lambda^2 (14 + t\lambda^2)$$

and

$$B(\lambda) := 24 - (9 - 8t + 3\sqrt{9 - 8t}) \lambda^2.$$

The sign of $N[w]$ on $0 < r < \infty$ is determined by the sign of $C(r; \lambda)$, which in turn is determined by the signs of $A(\lambda)$ and $B(\lambda)$.

For $\lambda > 0$ (and $t < 0$), we have

$$A(\lambda) \geq 0 \Leftrightarrow \lambda \leq \sqrt{\frac{14}{-t}} =: \lambda_A,$$

and $B(\lambda) \geq 0 \Leftrightarrow$

$$\lambda \leq \sqrt{\frac{24}{9 - 8t + 3\sqrt{9 - 8t}}} = \sqrt{\frac{6}{\sqrt{9 - 8t}} \frac{1}{h_+}} =: \lambda_B.$$

These satisfy $\lambda_B < \lambda_A$, for all $t < 0$. We conclude that $N[w] \geq 0$, for $0 < r < \infty$, if $\lambda \leq \lambda_B$, and $N[w] \leq 0$, if $\lambda \geq \lambda_A$. We can therefore take $\alpha(r) := w(r; \lambda_A)$ and $\beta(r) := w(r; \lambda_B)$ to obtain the expressions in (8).

We would like to conclude that there exists a solution to (A1) satisfying $\alpha(r) \leq h(r) \leq \beta(r)$. Such results are classical for *regular* problems on *finite* intervals. They can also be extended to problems with certain types of end-point singularities and/or on infinite intervals. We were not able to find a reference that covered our exact problem, and so we include here (for completeness) a proof of this in our case.

The following version of the classical result is taken from [11] and, though not the strongest statement possible, is adequate for our purposes. Consider the general problem

$$x'' = f(t, x, x'), \quad a < t < b,$$

$$x(a) = A, \quad x(b) = B,$$

with $-\infty < a < b < \infty$. Make the following hypotheses:

1. There exist functions $\alpha, \beta \in C^2(a, b) \cap C[a, b]$ satisfying $\alpha(t) \leq \beta(t)$, $\alpha'' \geq f(t, \alpha, \alpha')$, $\beta'' \leq f(t, \beta, \beta')$, for $a < t < b$, plus $\alpha(a) \leq A \leq \beta(a)$ and $\alpha(b) \leq B \leq \beta(b)$.
2. The function f is continuous on the set

$$S := \{(t, x, y) \mid a \leq t \leq b, \alpha(t) \leq x \leq \beta(t), y \in \mathbb{R}\}.$$

3. The function f is uniformly Lipschitz continuous with respect to y on S , that is, there exists a constant L such that for all $(t, x, y_1), (t, x, y_2) \in S$,

$$|f(t, x, y_2) - f(t, x, y_1)| \leq L |y_2 - y_1|.$$

Under these conditions, we are guaranteed that (A1) has a solution $x \in C^2(a, b) \cap C[a, b]$ satisfying $\alpha(t) \leq x(t) \leq \beta(t)$ and $|x'(t)| \leq M$, for $a < t < b$, where the constant M depends only on the set S (which is determined by $a, b, \alpha(t)$, and $\beta(t)$) and the Lipschitz constant L .

We adapt the argument of [11, Th. 1.7.1] and consider our singular, semi-infinite problem as a limit of regular, finite problems, to which the result above applies. Starting from an arbitrary $0 < a_1 < b_1 < \infty$, construct a nested sequence of finite intervals $I_n := [a_n, b_n]$ the end-points of which monotonically approach the limits $a_n \rightarrow 0$ and $b_n \rightarrow \infty$, as $n \rightarrow \infty$. For each positive integer n , let $h_n(r)$ be the solution to the problem $N[h_n] = 0$, $a_n < r < b_n$,

$$h_n(a_n) = \frac{\alpha(a_n) + \beta(a_n)}{2}, \quad h_n(b_n) = \frac{\alpha(b_n) + \beta(b_n)}{2}.$$

It follows from the result quoted above that such a solution exists and satisfies $\alpha(r) \leq h_n(r) \leq \beta(r)$, $|h'_n(r)| \leq M_n$, for $a_n \leq r \leq b_n$, where the constant M_n depends only on $\alpha(r)$, $\beta(r)$, a_n , and b_n .

Now the entire sequence $\{h_n\}$ is defined on the initial (innermost) interval I_1 . Moreover, $\{h_n\}$ and $\{h'_n\}$ are *uniformly bounded* there. In addition, $\{h_n\}$ and $\{h'_n\}$ are *equicontinuous* on I_1 ; this follows from the following mean-value estimations (which are valid for some $\rho, \rho' \in I_1$):

$$|h_n(r_2) - h_n(r_1)| = |h'_n(\rho)||r_2 - r_1| \leq M_1|r_2 - r_1|$$

and

$$\begin{aligned} |h'_n(r_2) - h'_n(r_1)| &= |h''_n(\rho')||r_2 - r_1| \\ &= |f(\rho', h_n(\rho'), h'_n(\rho'))||r_2 - r_1| \\ &\leq M'_1|r_2 - r_1|. \end{aligned}$$

Here we use $f(r, h, h')$ to denote the right hand side of the differential equation (A1) when written in the general explicit form $h'' = f(r, h, h')$. We have also used the fact that the point $(\rho, h_n(\rho), h'_n(\rho))$ lies in a closed bounded set, determined by the inequalities

$$a_1 \leq \rho \leq b_1, \quad \alpha(\rho) \leq h_n(\rho) \leq \beta(\rho), \quad -M_1 \leq h'_n(\rho) \leq M_1,$$

on which f is continuous, and so $|f|$ can be bounded by a constant, which above we call M'_1 .

We conclude, by the theorem of Arzelà and Ascoli characterizing compactness in spaces of continuous functions, that there must exist a subsequence, call it $\{h_{1,k}\}$, and limiting function h such that $h_{1,k} \rightarrow h$ and $h'_{1,k} \rightarrow h'$, as $k \rightarrow \infty$, uniformly on I_1 . The function h will be in $C^2(a_1, b_1) \cap C[a_1, b_1]$ and will satisfy $N[h] = 0$ and $\alpha(r) \leq h(r) \leq \beta(r)$, for $a_1 < r < b_1$.

Proceeding now to the next interval, I_2 , one can extract from $\{h_{1,k}\}$ a subsequence $\{h_{2,k}\}$ that converges similarly on I_2 , to an extension of $h(r)$. We continue in this way. The “diagonal sequence” $\{h_{k,k}\}$ will converge uniformly in C^1 on any compact subset of $(0, \infty)$ to a solution of $N[h] = 0$ satisfying $\alpha(r) \leq h(r) \leq \beta(r)$. It follows that this maximally extended function satisfies $h \in C^2(0, \infty)$, $N[h] = 0$ and $\alpha(r) < h(r) < \beta(r)$ on $0 < r < \infty$, $\lim_{r \rightarrow 0^+} h(r) = 0$, and $\lim_{r \rightarrow \infty} h(r) = h_+$.

**APPENDIX B: REGION OF VALIDITY OF MAXIMUM PRINCIPLE AND ITS
CONSEQUENCES**

Consider the limiting rescaled problem

$$\begin{aligned} \hbar'' + \frac{2}{\bar{r}} \hbar' - \frac{6}{\bar{r}^2} \hbar + \hbar - \hbar^3 &= 0, \quad 0 < \bar{r} < \infty, \\ \hbar(0) &= 0, \quad \hbar(\infty) = 1. \end{aligned} \tag{B1}$$

From our previous differential-inequality arguments, it follows that this problem has a positive solution, $\hbar_\infty(\bar{r})$, that satisfies

$$\bar{\alpha}_\infty(\bar{r}) = \frac{\bar{r}^2}{\bar{r}^2 + 14} \leq \hbar_\infty(\bar{r}) \leq \frac{\bar{r}^2}{\bar{r}^2 + 3} = \bar{\beta}_\infty(\bar{r}).$$

This solution (and upper bound) were used in the metastability analysis. Now the problem (B1) is nonlinear, and it is possible that there may be other solutions to it. We show here that these other potential solutions are pointwise bounded in magnitude by $|\hbar_\infty(\bar{r})|$, and so the earlier metastability analysis remains valid for *any* solution of (B1). We also obtain that $\hbar_\infty(\bar{r})$ is unique within a certain restricted class. The arguments rely on classical maximum principles.

Suppose $\hbar_1(\bar{r})$ and $\hbar_2(\bar{r})$ are any two solutions of (B1). Then their difference, $\bar{e} := \hbar_2 - \hbar_1$, satisfies

$$\bar{e}'' + \frac{2}{\bar{r}} \bar{e}' - \frac{6}{\bar{r}^2} \bar{e} + \bar{e} - (\hbar_2^3 - \hbar_1^3) = 0, \quad \bar{e}(0) = \bar{e}(\infty) = 0. \tag{B2}$$

Applying the Mean Value Theorem to the nonlinear term, this can be written

$$\bar{e}'' + \frac{2}{\bar{r}} \bar{e}' + \left[-\frac{6}{\bar{r}^2} + 1 - 3\bar{\eta}^2(\bar{r}) \right] \bar{e} = 0,$$

for some intermediate value $\bar{\eta}(\bar{r})$, which must satisfy

$$\min \{ \hbar_1(\bar{r}), \hbar_2(\bar{r}) \} \leq \bar{\eta}(\bar{r}) \leq \max \{ \hbar_1(\bar{r}), \hbar_2(\bar{r}) \}.$$

A classical maximum/minimum principle will apply to solutions of this equation if the term in brackets can be shown to be *negative*, i.e., where

$$1 - \frac{6}{\bar{r}^2} \leq 3\bar{\eta}^2(\bar{r}).$$

The region where this is valid is depicted in Figure 7.

We can see (and it can be proven rigorously to be the case) that the lower-bounding solution $\bar{\alpha}_\infty(\bar{r})$ and its negative are both completely contained in this region and so then will be $\pm\bar{h}_\infty(\bar{r})$. As a consequence, if $\bar{h}_2(\bar{r})$ is any other potential solution of (B1), then $\bar{h}_2 - \bar{h}_\infty$ cannot have a positive interior maximum, and $\bar{h}_2 + \bar{h}_\infty$ cannot have a negative interior minimum. It follows that we must have

$$|\bar{h}_2(\bar{r})| \leq |\bar{h}_\infty(\bar{r})|, \quad 0 \leq \bar{r} < \infty.$$

Thus the metastability analysis of Section IV is valid (for finite R and t as well, by continuity) for *any* potential solution of (B1).

Since the region of validity of the Maximum Principle does *not* contain the entire $0 < \bar{r} < \infty$ half plane, we are unable to preclude the possibility of another potential solution (different from $\bar{h}_\infty(\bar{r})$) having a portion of its graph in the region $3\bar{\eta}^2 < 1 - 6/\bar{r}^2$ (where a maximum/minimum principle need not be valid) and having its maximum difference from $\bar{h}_\infty(\bar{r})$ there. All that can be said then, using these somewhat simple tools, is that $\bar{h}_\infty(\bar{r})$ is unique within the class of functions whose values are restricted to the region $3\bar{\eta}^2 \geq 1 - 6/\bar{r}^2$, where the classical Maximum Principle applies.

REFERENCES

- [1] N. Schopohl and T. J. Sluckin, *J. Phys. France* **49**, 1097 (1988).
- [2] E. Penzenstadler and H.-R. Trebin, *J. Phys. France* **50**, 1027 (1989).
- [3] A. Sonnet, A. Kilian, and S. Hess, *Phys. Rev. E* **52**, 718 (1995).
- [4] R. Rosso and E. G. Virga, *J. Phys. A: Math. Gen.* **29**, 4247 (1996).
- [5] O. D. Lavrentovich and E. M. Terentjev, *Zh. Éksp. Teor. Fiz.* **91**, 2084 (1986), [*Sov. Phys. JETP* **64**, 1237 (1986)].
- [6] R. Cohen and M. Taylor, *Comm. Partial Differential Equations* **15**, 675 (1990).
- [7] C. Chiccoli *et al.*, *J. Phys. II France* **5**, 427 (1995).
- [8] L. Longa, D. Monselesan, and H.-R. Trebin, *Liq. Cryst.* **2**, 769 (1987).
- [9] T. A. Davis and E. C. Gartland, Jr., *SIAM J. Numer. Anal.* **35**, 336 (1998).
- [10] S. Mkaddem, Ph.D. thesis, Department of Mathematics and Computer Science, Kent State University, 1998.
- [11] S. R. Bernfeld and V. Lakshmikantham, *An Introduction to Nonlinear Boundary Value Problems* (Academic Press, Inc., New York and London, 1974).
- [12] J. Schröder, *Operator Inequalities* (Academic Press, New York, London, Toronto, Sydney, San Francisco, 1980).

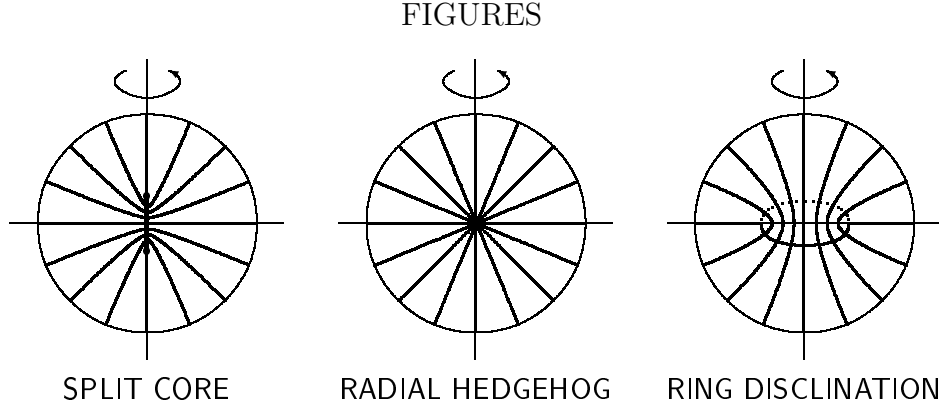


FIG. 1. Three equilibrium director profiles in a radially aligned spherical nematic droplet.

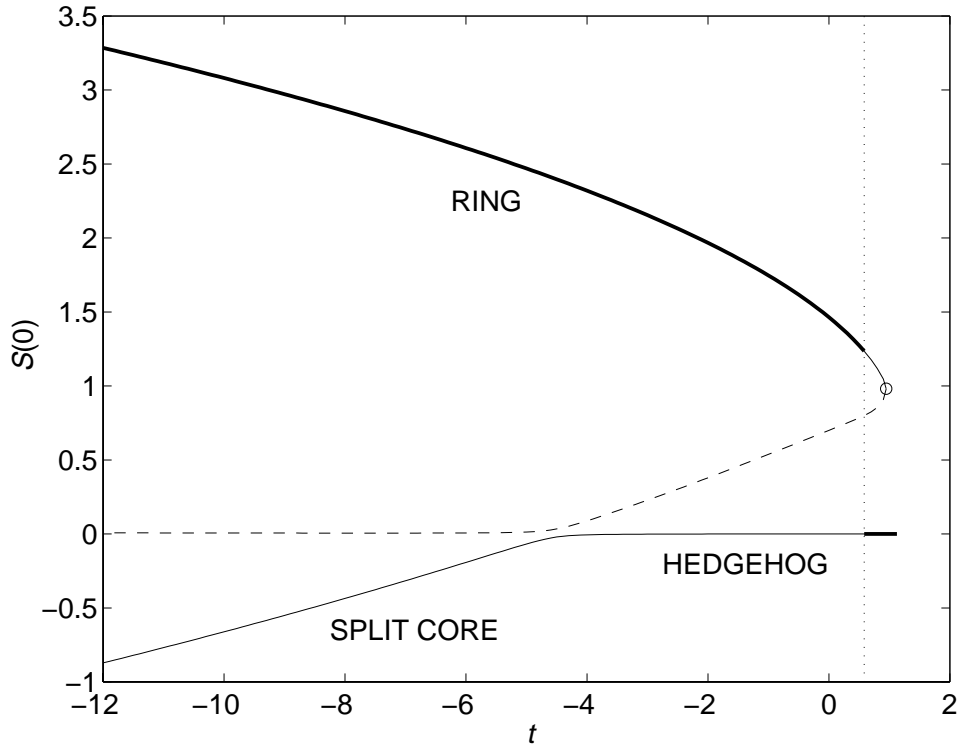


FIG. 2. Bifurcation diagram of discretized model for Split Core, Radial Hedgehog, and Ring Disclination configurations. Scalar order parameter at the center ($S(0)$) vs reduced temperature (t). Bold line indicates *stable* equilibrium (minimum free energy); solid line indicates *metastable* (locally stable); dashed line indicates *not metastable* (locally unstable). Vertical dotted line indicates *transition temperature*: below this temperature, the *Ring Disclination* (uppermost branch) has minimum free energy; while above it, the free energy of the *Radial Hedgehog* (isotropic at the origin) is the global minimum.

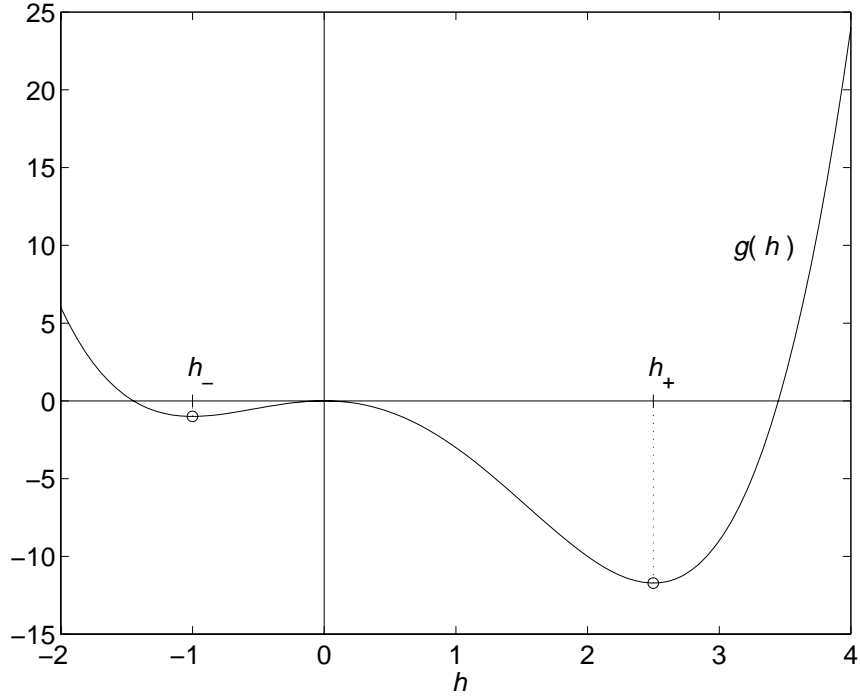


FIG. 3. Bulk potential $g(h) = -th^2/2 - h^3 + h^4/2$ for radial hedgehog free energy at reduced temperature $t = -5$.

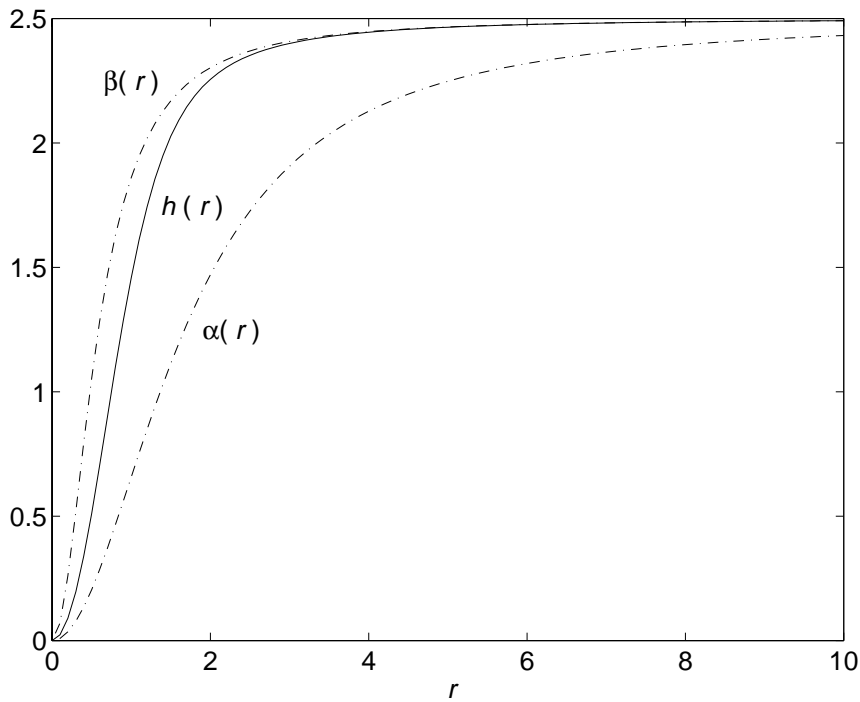


FIG. 4. Analytic upper and lower bounds for radial hedgehog solution $h(r)$ at reduced temperature $t = -5$.

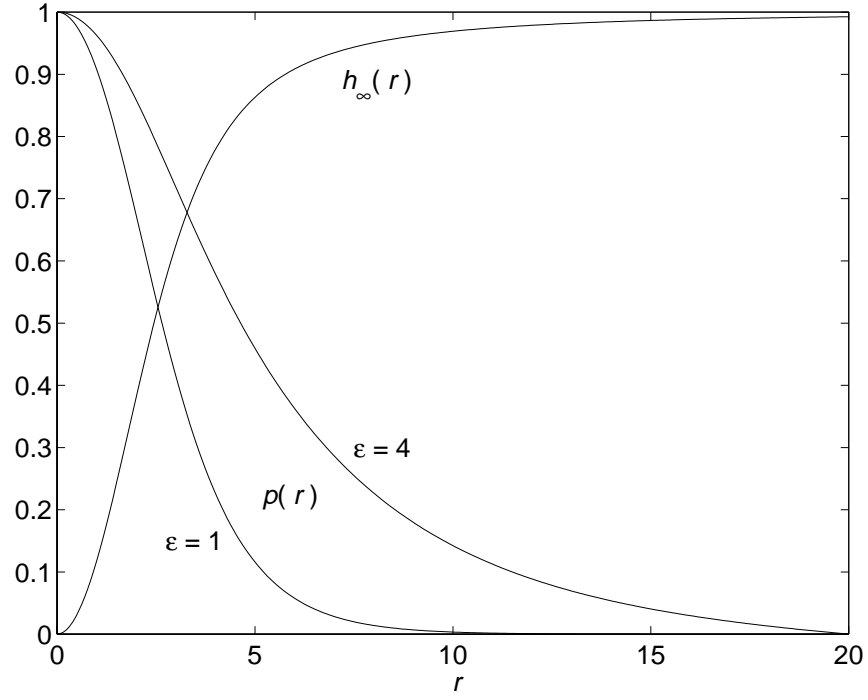


FIG. 5. Limiting rescaled form of radial hedgehog solution (“inner solution”) $\tilde{h}_\infty(\bar{r})$ versus the minimum eigenmode $\bar{\rho}(\bar{r})$ in the local instability criterion for two cases of the coupling coefficient: $\epsilon = 1$ and $\epsilon = 4$.

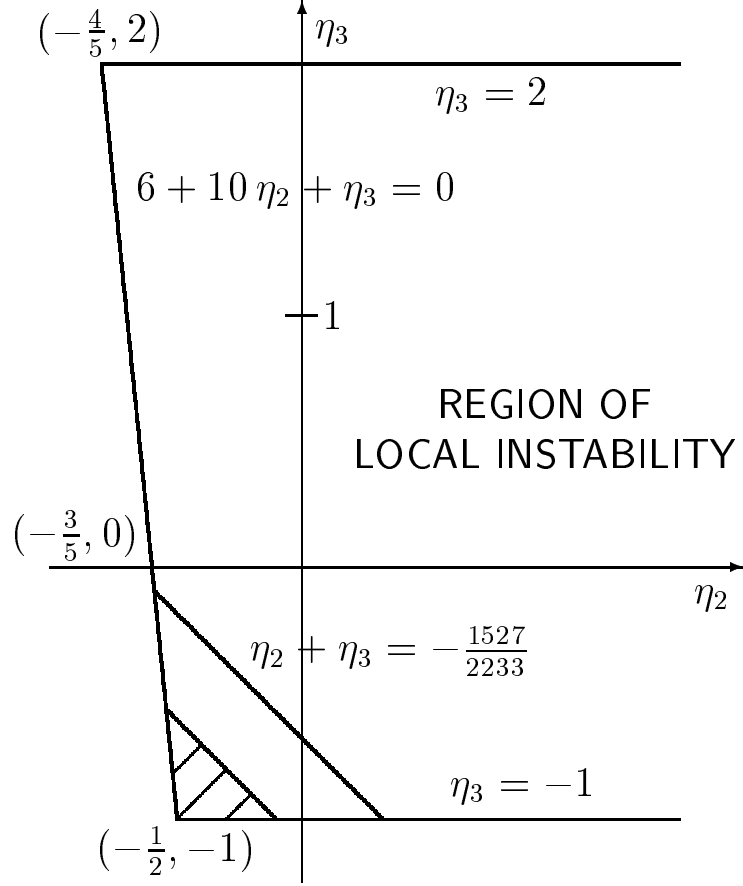


FIG. 6. Region of local instability for radial hedgehog configuration in terms of elastic-constant ratios $\eta_2 = L_2/L_1$, $\eta_3 = L_3/L_1$. The hedgehog is proven here not to be metastable throughout the entire admissible range ($-1 < \eta_3 < 2$, $6 + 10\eta_2 + \eta_3 > 0$) with the exception of the hashed region near the lower left corner above. Analytical bounds are sufficient to produce the outer enclosure $\eta_2 + \eta_3 \leq -1527/2233$ of this excluded portion.

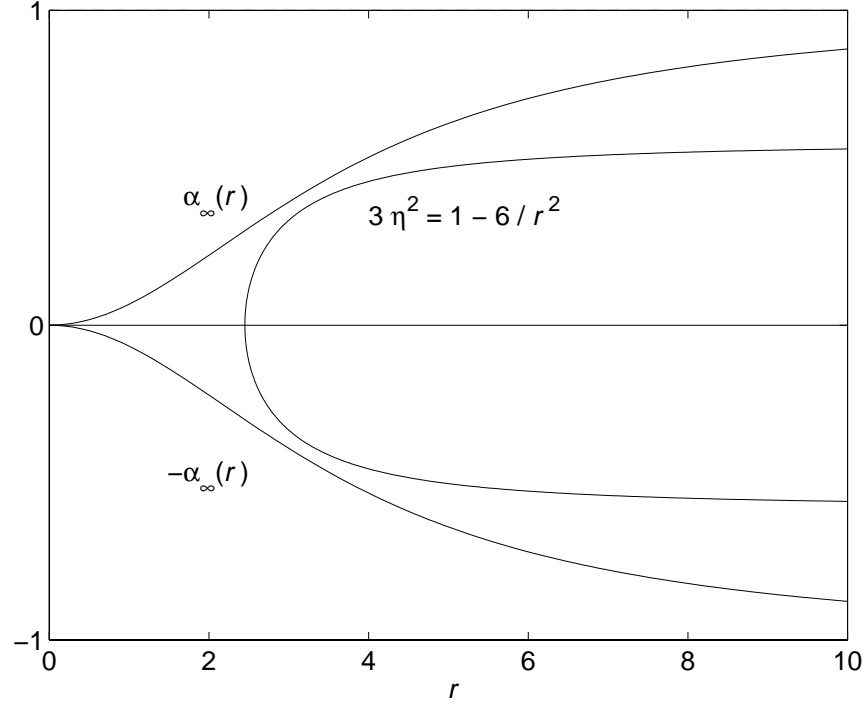


FIG. 7. Region of validity of Maximum Principle for linearized error equation (B2) compared to $\bar{\alpha}_\infty(\bar{r})$, the analytical lower bound for the limiting rescaled hedgehog solution $\bar{h}_\infty(\bar{r})$. The classical Maximum Principle holds outside the region enclosed by the curve $3\bar{\eta}^2 = 1 - 6/\bar{r}^2$, which contains the graphs of $\pm\bar{\alpha}_\infty(\bar{r})$ and, as a consequence, $\pm\bar{h}_\infty(\bar{r})$.